

The structure of shear bands in twinned fcc crystals and their influence on recrystallization nucleation

H. PAUL^{1*} and J.H. DRIVER²

¹Institute of Metallurgy and Materials Science, Polish Academy of Sciences, 25 Reymonta St., 30-059 Cracow, Poland

²Ecole Nationale Supérieure des Mines de Saint Etienne, Centre SMS, 158 Cours Fauriel, 42023 Saint Etienne, Cedex 2, France

Abstract. The orientations of recrystallization nuclei and their adjacent as-deformed regions have been characterised in deformed single crystals of different metals (Ag, Cu, Cu-2%wt.Al and Cu-8%wt.Al) in which twinning and/or shear banding occur. $\{112\}\langle 111 \rangle$ oriented crystals of these metals have been compressed to different strains, then lightly annealed, and the crystallographic aspects of the recrystallization process along shear bands examined by local orientation measurement in TEM and SEM.

The results clearly show the existence of a well-defined crystallographic relation between the local deformation substructure and the first recrystallized areas of uniform orientation. The first-formed nuclei always exhibit near $25\text{--}40^\circ$ ($\langle 111 \rangle$ — $\langle 112 \rangle$) type misorientations, in the direction of highest growth, with respect to one of the two main groups of the deformation texture components. The rotation axes can be correlated with the slip plane normal of highest activity. As recrystallization proceeds, recrystallization twinning develops strongly and facilitates rapid growth; the first and higher generations of twins then tend to obscure the initial primary crystallographic relation between the shear bands and recrystallization nuclei.

Key words: nucleation of recrystallization, texture, electron diffraction, single crystals.

1. Introduction

One of the major problems of recrystallization is characterizing and understanding the influence of the orientations present in the deformed state on the nucleation process. On annealing highly deformed fcc metals, a strong recrystallization texture is usually found, which may involve the partial retention of the deformation texture, but quite often a very different but very strong new texture forms [1]. Two major alternative models exist for the formation of a strong new texture, usually described as 'orientation nucleation' (ON) or 'oriented growth' (OG). The ON model is the hypothesis that grains, with an orientation that dominates the fully recrystallized texture, nucleate more frequently than do grains of all other orientations. In other words, it is assumed that the preferred formation of special orientations determines the final recrystallization texture [2]. On the contrary, the OG model assumes that grains with particular orientation attain sizes significantly larger than the average diameter of the recrystallized grains [3]. The basis for such an approach have been the observations of high mobilities of recrystallization fronts of certain misorientations. The well-known work by Liebmann et al [3], and more recently by Molodov et al [4] have proved that misorientations across grain boundaries of $40^\circ\langle 111 \rangle$ -type depict maximum mobility in fcc metals [5]. These models describe the phenomenon of the recrystallization texture quantitatively, but totally leave determination of the mechanisms giving rise to the effects.

In this paper, the influence of specific microtexture components of the deformed state on the orientations of the first recrystallized nuclei, together with the misorientations at the recrystallisation front will be addressed in detail. From the

crystallographic point of view, physical intuition suggests that the starting points for the occurrence of 'new' orientations are the components of the as-deformed state, i.e. the orientation of each new grain arises from nearly the same orientation present in the deformed state. Thus, what makes these new grains grow from small, recovered sub-grains or sub-cells that are already present in the deformation microstructure and what kind of dislocation mechanism controls this process?

The current study is aimed at investigating the influence of shear band internal microtexture components on recrystallization nuclei orientations. For this purpose, channel-die deformed $(112)[11\bar{1}]$ single crystal samples of different low SFE metals, i.e. Cu-2%Al, Cu-8%Al and silver, deformed at 293 K as well as copper deformed at 77 K to well-developed twin matrix layered structures, were examined. Earlier work [1,6–16] has clearly shown that the analysis of nucleation, growth and recrystallization twinning in polycrystalline metals is very complicated because of the large number of microstructural and microtextural factors that influence this process. Therefore, in the present study, the recrystallization behaviour of plane strain compressed single crystals was analysed. The copper of $C(112)[11\bar{1}]$ orientation was chosen, since these crystals exhibit a strong tendency to undergo shear banding. The bands lie along a plane parallel to the transverse direction (TD) and penetrate the whole volume of the sample (see e.g. [17]). They are usually grouped into clusters, which make up macroscopically visible shear bands. The use of crystals with clearly defined shear bands also allows one to investigate the orientations of recrystallization nuclei growing along these highly localised deformation microstructures and obviously eliminates the pos-

*e-mail: nmpaul@imim-pan.krakow.pl

sibility of nucleation along grain or twin boundaries and other types of inhomogeneities. In addition, the annealing conditions can be chosen to limit recrystallization to the shear band area and hence simplify the investigation of the crystallographic correlation between the deformed and the recrystallized states.

2. Experimental procedures

High purity single crystals of silver, Cu, Cu-2%Al and Cu-8%Al with C(112)[11 $\bar{1}$] initial orientation, obtained by the Bridgman method, were prepared in the form of 10×10×10 mm cubes. The samples were deformed at room temperature (in the case of pure copper the samples were deformed at 77 K) in a TeflonTM lubricated channel-die, using multi-stage tests to form SBs and their compact clusters called macroscopic shear bands (MSB). They were then annealed in an air furnace for 30 s at temperatures of 265–300°C for silver and for 60 s at 460°C for copper and copper base alloys. These treatments develop partial recrystallization only within regions confined to MSB.

The detailed microtexture evolutions during recrystallization nucleation and growth were analysed by modern techniques using TEM and SEM. For nanoscale analyses the local orientations were characterized by TEM using a 200 kV PHILIPS CM200 with semi-automated Kikuchi line based analysis. The thin TEM foils were prepared by a twin-jet technique in standard methanol – nitric acid solution. TEM methods were used to examine the dislocation substructure in relation to changes in microtexture in the as-deformed and partly recrystallized samples. Microstructure observations and systematic local orientation measurements were also examined in a JEOL 6400 SEM and JSM 6500F equipped with field emission gun (FEG), using backscattered electrons at 20 kV to reveal crystallographic contrast. The SEM was equipped with facilitates for EBSD (Electron Backscattered Diffraction). Microscope control, pattern acquisition and solution were carried out with the HKL Channel 5 system. In all cases a step size of 0.1 μm – 1 μm was applied. For more global (sample scale) microstructure observations optical microscopy was used on mechanically and chemically polished samples.

Local orientation data, obtained by TEM and SEM on the ND-ED plane (where: ND – normal direction, ED – extension/rolling direction) were transformed to the standard ED-TD reference system and presented in the form of {111} pole figures and/or distributions of the misorientation axes.

3. Results

3.1. The shear band structures and textures. General remarks. The matrix and SB structures and microtextures have been previously reported in detail [2–5]. Fine (0.1 μm) twin matrix (T-M) lamellae are formed rapidly (in all metals) in the early stages of deformation, such that the twins very quickly tend to occupy a significant volume of the crystals.

Well-developed SBs observed by TEM are exemplified by the broad SB of Fig. 1a, formed against a background of T-M plates situated parallel to the compression plane, in a silver single crystal of C(112)[11 $\bar{1}$] – initial orientation, channel-die deformed 67%. The orientations of the T-M layers outside the

band can be described by two sets very close to: (111)[11 $\bar{2}$]^M + (111)[$\bar{1}\bar{1}2$]^T, for the matrix and for the twins, respectively, describing also the situation shown in Fig. 1b and 1c. At the SB boundary this T-M layered structure changes inclination, varying from 20° to about 30° to ED, indicating a gradual incorporation of the structure outside the band into the band. This is clearly visible at the early stages of SB formation as a result of reduced stability within narrow zones. 1–2 μm thick SBs, inclined at 40–42° to ED, are formed at moderate deformations. The microstructure of a well-developed SB is composed of very fine sub-grains, highly elongated along the shear direction. The orientations characteristic of the twinned matrix and SB are presented in Figs. 1b and c respectively. For all these orientations, TD is parallel to the <110> direction. They are grouped within a broad range of orientations from {111}<112> to {110}<001>, with strong scattering mainly around (+/-)TD (Fig. 1c) and show the lack of the matrix orientation. The maximum density of the band orientations is near G{110}<001> and results from the 15–30° (+)TD rotations of areas associated with the twins outside the SB. However, the interpretation of the real lattice re-orientation within SB is more complex than this simple TD rotation. TEM orientation line scans (Fig. 1d) within the SB reveal large orientation spreads of up to 35–40°; most of these misorientations occur about the TD||<110> axis, but at these high strains there are significant further rotations about one of the two <112> poles close to TD. This is the basis of the suggestion by Paul et al. [17,18] that slip on the two co-planar slip systems in the band becomes progressively asymmetric, i.e. the rotation about one of the two <112> poles corresponds to local slip on one of the two {111}<110>-type slip systems. It is this localized asymmetric slip which reorients the initial near-Goss shear band to the S-B components.

3.2. TEM orientation mapping. The availability of local orientation determination with high spatial resolution created the opportunity to formulate and verify the mechanisms of lattice rotations. This was done by looking into subtle orientation changes within a SB itself as well as at the boundary between the band and the twinned matrix. TEM observations reveal the deflection of the T-M layers in sparsely spaced narrow zones of the material. Roughly, in C-oriented single crystals, this process is associated with the rotation about TD||<110> direction.

The TEM bright field microstructure of the area where T-M layers are crossed by a SB in 50% channel-die deformed copper at 77K is shown in Fig. 2a. Here, twin boundaries in the matrix are inclined by 22°–25° to ED, whereas the angle between the shear band plane and the compression plane is in the range 40°–42°. Figure 2a also shows that the position of the elongated sub-cells forming the structure of the shear band is nearly parallel to the SB direction. A similar area is covered by the TEM orientation map given in Fig. 2b. This 2 μm x 2 μm image was created with the step size of 20 nm. The map reflects microtextures of the twinned matrix and a SB. Points corresponding to unsolved or incorrectly indexed patterns (~12% of points in Fig. 2b) are white. Orientations at points constituting the map are represented in the {111} pole figure (Fig. 2c). The figure shows that the scattering of orientations is mainly due to the rotation about TD||<110>. Two groups of orienta-

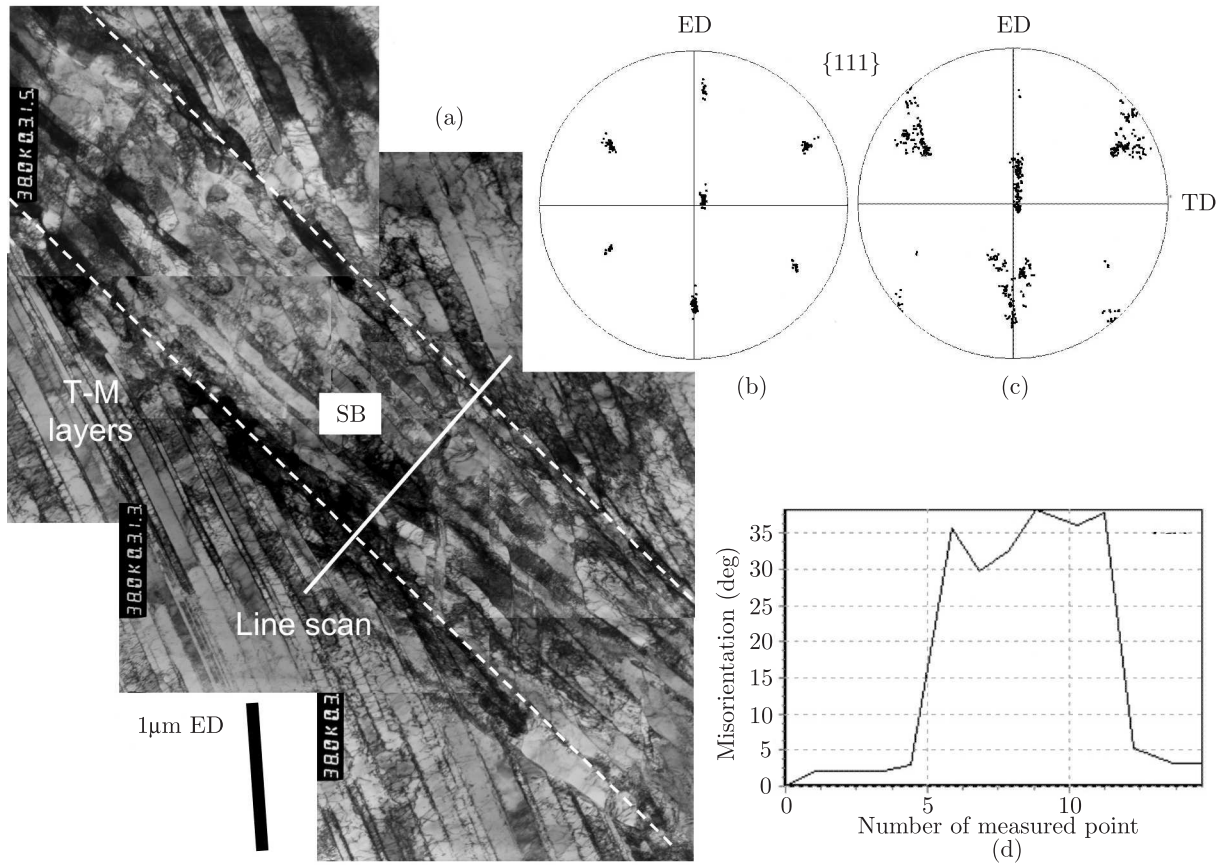


Fig. 1. (a) TEM microstructure showing an advanced stage of shear band formation against a background of the compact twin-matrix layer structure after 67% compression. (b) and (c) $\{111\}$ pole figures from areas of the twinned matrix (outside the band) and the SB, respectively. (d) Misorientation profile with respect to the first measured point, along the line scan across the SB presented in (a). TEM local orientation measurements

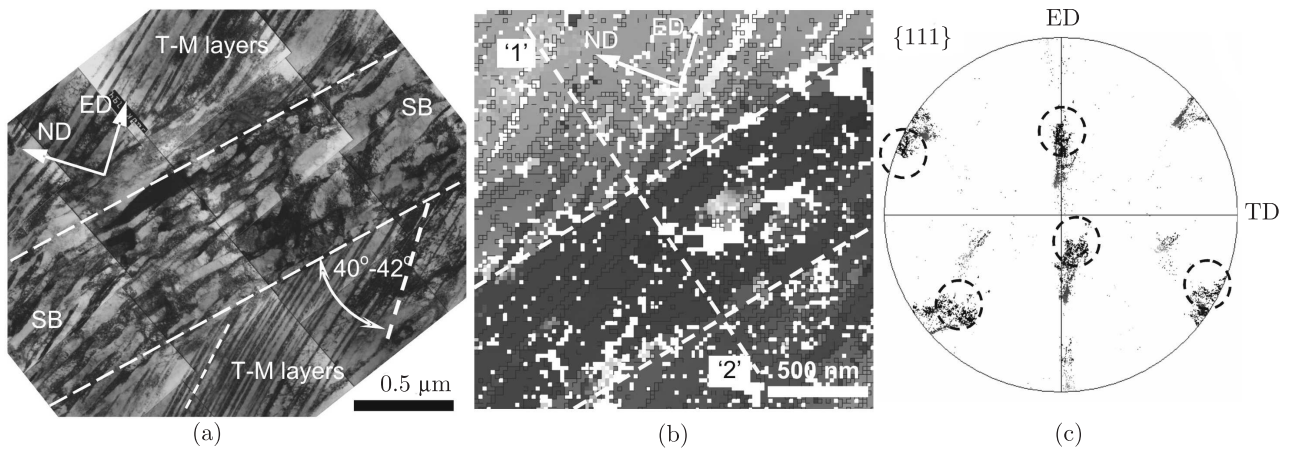


Fig. 2. (a) TEM microstructure of copper deformed 50% at 77 K. A broad shear band developed against a background of compact twin-matrix layers. (b) TEM orientation map obtained with 20nm step size. Orientations at points marked in white were not determined, and (c) corresponding $\{111\}$ pole figure. Dashed circles mark orientations of SB area

tions are clearly visible. The first, weaker, with the average position near $\{114\}\langle 221 \rangle$ (G^T), originates from the primary matrix. The second (twin related to the first one) is spread around the Goss position. The orientations of the SB fall in the cir-

cles marked in Fig. 2c. Analysis of these figures indicates that a number of rotation types are responsible for scattering of the T-M orientations in the SB area. Besides the already mentioned rotation about $\langle 110 \rangle$, rotations about less specific axes

take place; the axes are spread towards $\langle 123 \rangle$ and $\langle 112 \rangle$ directions¹. These rotations are evident in essential parts of the discrete misorientation distribution function for the SB area where the scattering of misorientation axes between $\langle 110 \rangle$ and $\langle 112 \rangle$ directions is clearly visible [7,8,17,18]. Gradual orientation changes along the dashed line drawn across the band reach 35° with respect to the first point located outside the band and having the twin orientation (Fig. 3).

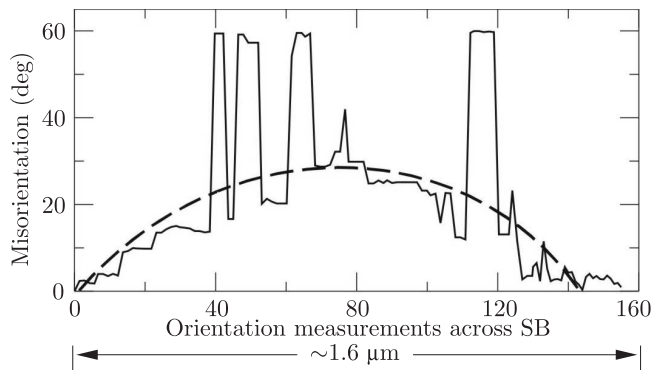


Fig. 3. Misorientations with respect to the first measured point, along an ED line scan presented in Fig. 5b (across the shear band) at 20 nm intervals. TEM local orientation measurements

3.3. General recrystallization behaviour. Figure 4 shows an example of a partly recrystallized microstructure obtained by optical microscopy in silver deformed 50% at 293 K and annealed for 40 s at 300°C . The lamellar structure of fine alternating T-M layers is crossed by compact clusters of SB usually inclined at $25\text{--}40^\circ$ to ED which constitute the nucleation sites of new, recrystallized grains. New grains are only formed in the MSB areas.

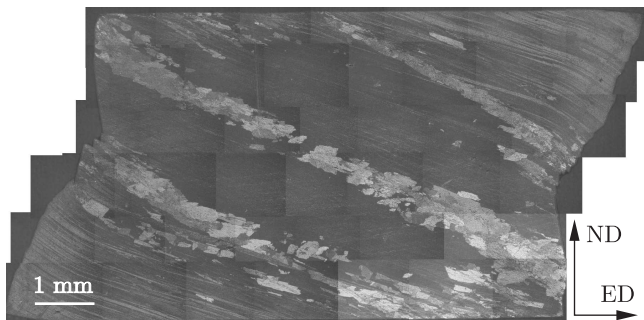


Fig. 4. Optical microstructure showing recrystallization within a SB. Silver deformed 50% at room temperature and after recrystallization for 40 s at 300°C

Twin boundaries ($\Sigma 3$, i.e. $60^\circ\langle 111 \rangle$), visible as bold, black lines on orientation maps, obtained by SEM/EBSD measurements (Fig. 5a and b) are developed within several recrystallized areas. There are, however, no recrystallized areas which are twin related to the deformed state. This observation suggests that recrystallization twinning (RT) is a secondary mechanism, associated with the growth of new grains, i.e. after

the formation of primary nuclei of uniform orientation. The global $\{111\}$ pole figure containing only the deformed state orientations is given in Figs. 5c and e and shows the matrix and twin orientations plus their spread due to SB formation. After short annealing the recrystallized grain orientations are represented by the $\{111\}$ pole figures in Figs. 5d and f; they show significant differences with respect to the as-deformed microtexture. However, there is a clear tendency for certain orientations (marked in the figure), situated at the limit of the range of the deformation microtexture, to participate in the nucleation process. In the as-deformed state, SB orientations are only weakly visible on the 'global' deformation texture and are located at the limit of their spread (at the (+)TD rotated boundary). In the early stages of primary recrystallization, some of the $\langle 111 \rangle$ poles become sharper. As recrystallization proceeds and $\alpha(\langle 111 \rangle\text{--}\langle 112 \rangle)$ rotations are developed in selected areas of the band, the intensity of the $\langle 111 \rangle$ pole of the most active $\{111\}$ planes during deformation systematically increases. This mechanism, as it will be demonstrated below, is in fact due to the retention of particular $\langle 111 \rangle$ poles of the deformed state in new positions, which correspond to the recrystallized grain.

3.4. Nucleation of new grains and the growth process. The nucleation and the subsequent recrystallization growth process occur in the same way for all the metals. In the present study only a strictly limited set of primary nucleus orientations was detected; all connected with $\alpha(\langle 111 \rangle\text{--}\langle 112 \rangle)$ -type rotations around selected axes [8]. A nucleus is considered to be a region of uniform orientation, typically $<1\ \mu\text{m}$ diameter, developed usually within a substructure of heavily dislocated and elongated cells (of width $\sim 0.2\text{--}0.5\ \mu\text{m}$). The micrograph in Fig. 6a was obtained at the initial nucleation stage within a SB area. Close to the new grain only one group of components oriented near $\{111\}\langle 112 \rangle$ with (+)TD scattering (Fig. 6b) was detected; this is the twin position within the old band rotated towards the compression plane. The orientation of the primary nucleus is therefore related to that of the as-deformed areas by $35\text{--}40^\circ(\langle 111 \rangle\text{--}\langle 112 \rangle)$ relations. All the misorientation axes are represented in Fig. 6c within one standard triangle. The preferential location of the rotation axes within the range of $\langle 111 \rangle\text{--}\langle 112 \rangle$ directions is clearly visible. Figure 6d shows a schematic pole figure for a transition from the as-deformed orientations to the nucleus orientation by rotation about $\langle 112 \rangle$ which is in quite good agreement with the observations. The value of the misorientation angle is confirmed by orientation scans across the grain, along the ED direction as given in Fig. 6e.

The case of a large grain growing preferentially along macroscopic clusters of SB observed at the TEM scale is illustrated in Fig. 7. It is apparent that the recrystallization front is very irregular, indicating different local growth rates due to local variation in the orientation relationship as a consequence of the orientation spread in the as-deformed areas, Fig. 7a.

¹However, only the rotation about $\langle 112 \rangle$ opens the possibility to provide a simple deformation mechanism based on the operation of the $\{111\}\langle 110 \rangle$ slip system.

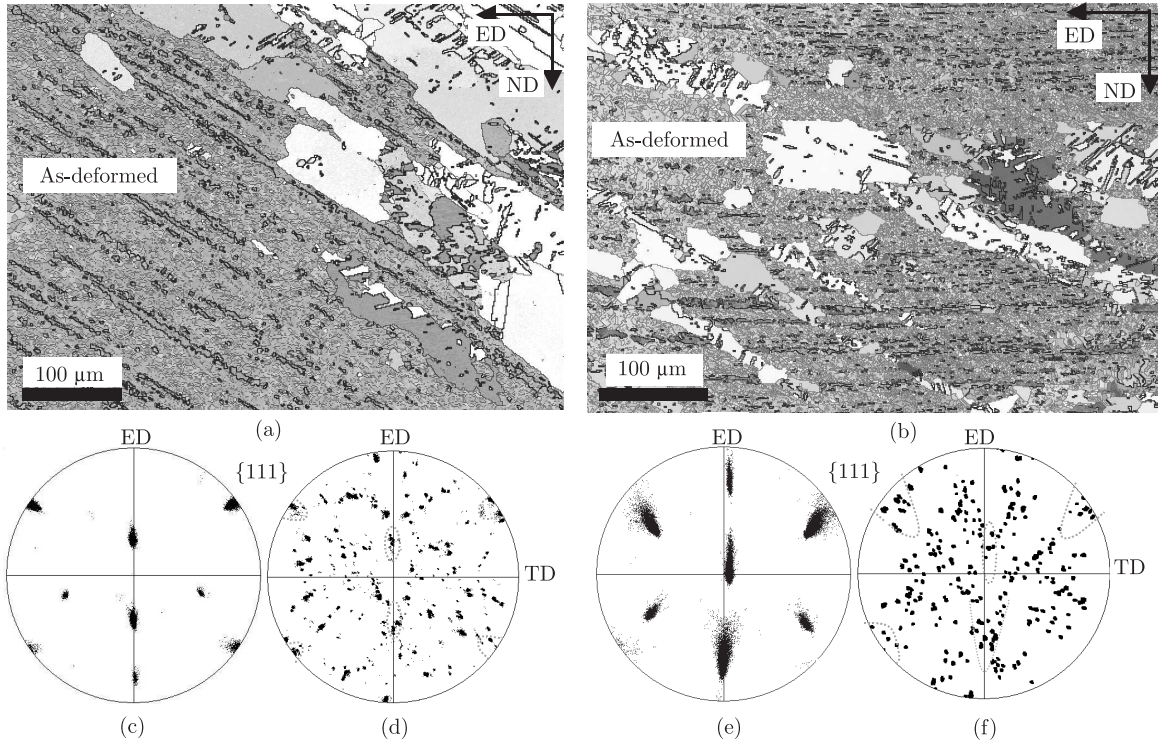


Fig. 5. Band contrast maps from SEM/EBSD measurements. Silver single crystal (a) deformed 32% and annealed for 30 s at 300°C and (b) deformed 67% and annealed for 30 s at 265°C. {111} pole figure from (c) and (e) as-deformed areas only and (d) and (f) recrystallized areas only, for the case presented in (a) and (b), respectively

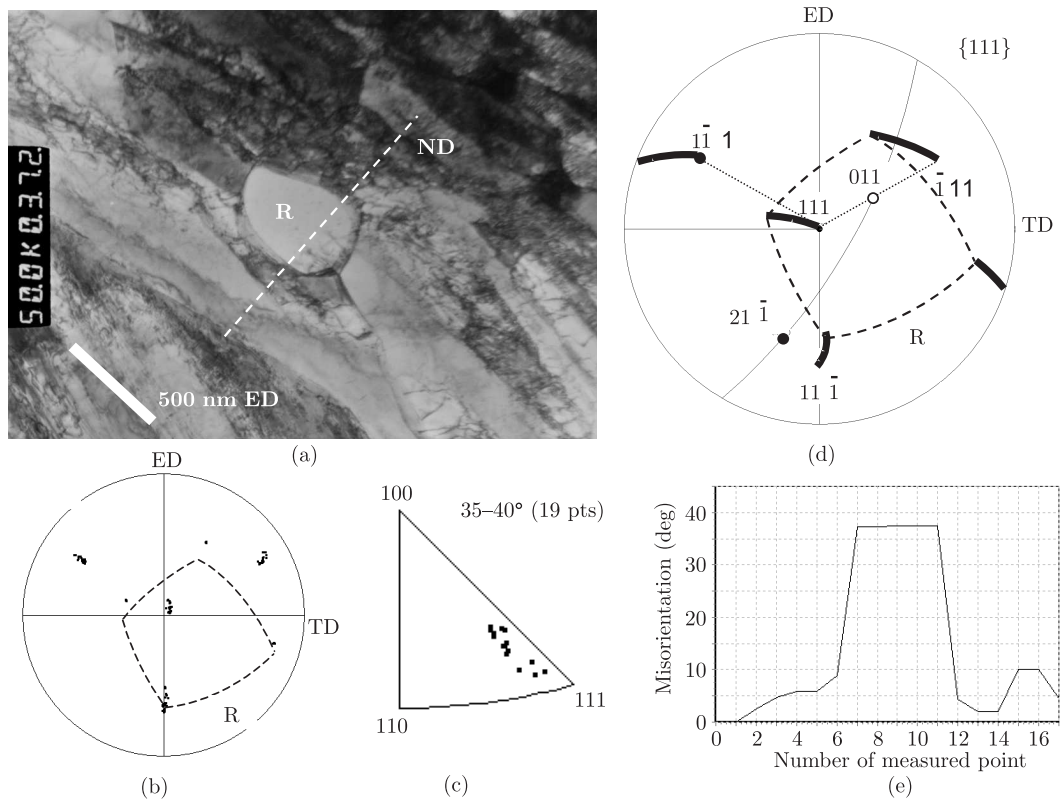


Fig. 6. Nucleation of new grain in Ag crystal deformed 67% and annealed 30 s at 285°C. (b) {111} pole figure containing orientations of the nuclei (R) and as-deformed area orientations. (c) the distribution of the misorientation axes between nuclei and nearest as-deformed neighbors. (d) stereographic projection showing transition from the orientation of the as-deformed areas towards nuclei orientation as a result of $\langle 112 \rangle$ type rotation. (e) misorientation profile across grain (parallel to ND). TEM local orientation measurements

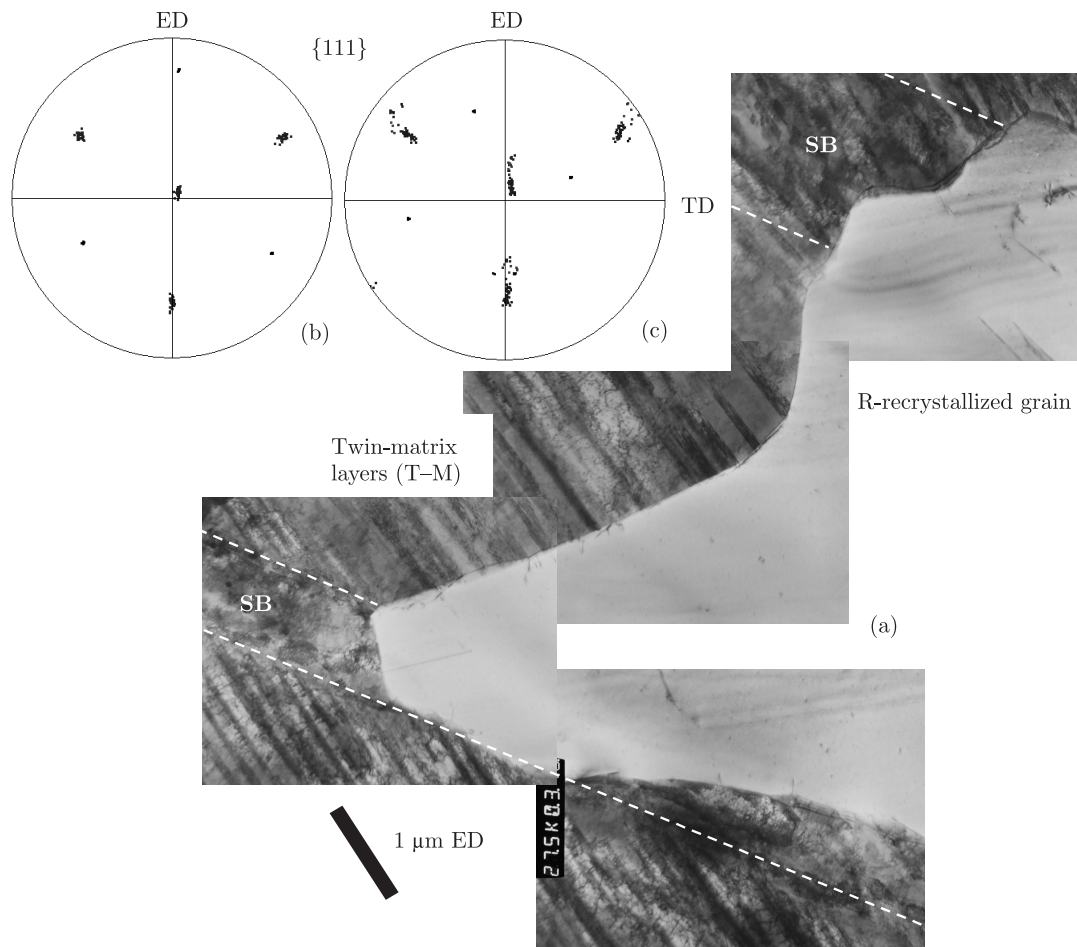


Fig. 7. Enlarged grain growing preferentially towards the thin SB in silver deformed 50% at 293 K and recrystallized for 30 s at 285°C. (a) TEM microstructure, and $\{111\}$ pole figures showing (b) the orientations of the twinned matrix outside the band, and (c) and recrystallized nucleus and neighbouring deformed areas within SB

A detailed TEM analysis of the orientation relations along the growth front indicates that the highest local growth rate (the part of recrystallized grain pulled forward) is connected with the additional strong lattice disturbance of the deformed structure within the band. The growing grain has a great tendency to consume these highly localized regions, resulting in an elongated shape along the band direction. It is evident that the shape of the recrystallization front results from its strong tendency to grow preferentially along the dislocation-rich layers within the bands. The segment of the grain boundary between white arrows (Fig. 7a) is considered the most mobile part. Here the orientation relation between the recrystallized grain and its nearest as-deformed neighbourhood (described again by the position of twins within the band) can be described as $25\text{--}35^\circ \langle 554 \rangle \text{--} \langle 311 \rangle$ for the part of grain pulled forward. In this case the migrating boundary of the growing grain is not stopped at the SB/twinned matrix boundary and it possesses a great tendency to consume also the T-M layers. The existence of the layered structure within the deformed state means that this orientation relationship with respect to one component of the deformation microtexture leads to another misorientation with respect to the other component, usually described as $50\text{--}55^\circ \langle uvw \rangle$. In the case of situation presented in Fig. 7a it

can be described by $40\text{--}50^\circ \langle 134 \rangle \text{--} \langle 253 \rangle$ -type misorientation for the part delayed in the growth process.

3.5. Recrystallization twinning. A more advanced stage of recrystallization (i.e. a grain with twins), observed in copper after 80% reduction at 77 K and annealed for 300 s at 265°C, is shown in Fig. 8a. A large grain, completely free of dislocations and containing twin-related areas, is characterised by the orientations shown in Fig. 8b as $\{111\}$ pole figures. The orientations of the neighbouring deformed areas are displayed in Fig. 8c, where the scattering of the D^M and D^T components is clearly observed. This is evidence that the orientation of the recrystallized area R has a common pole with the D^T oriented areas of the deformed state. The misorientations between recrystallized areas and the adjacent deformed regions within the SB are very close to $30^\circ \langle 111 \rangle$. This grain possesses a strong tendency to grow into the T-M layers rich in thin, freshly formed SB, inclined at about 35° to ED. It is also clear that during recrystallization nucleation only a very limited number of new recrystallized orientations are found and recrystallization twinning always occurs after the primary nucleus of uniform orientation formation.

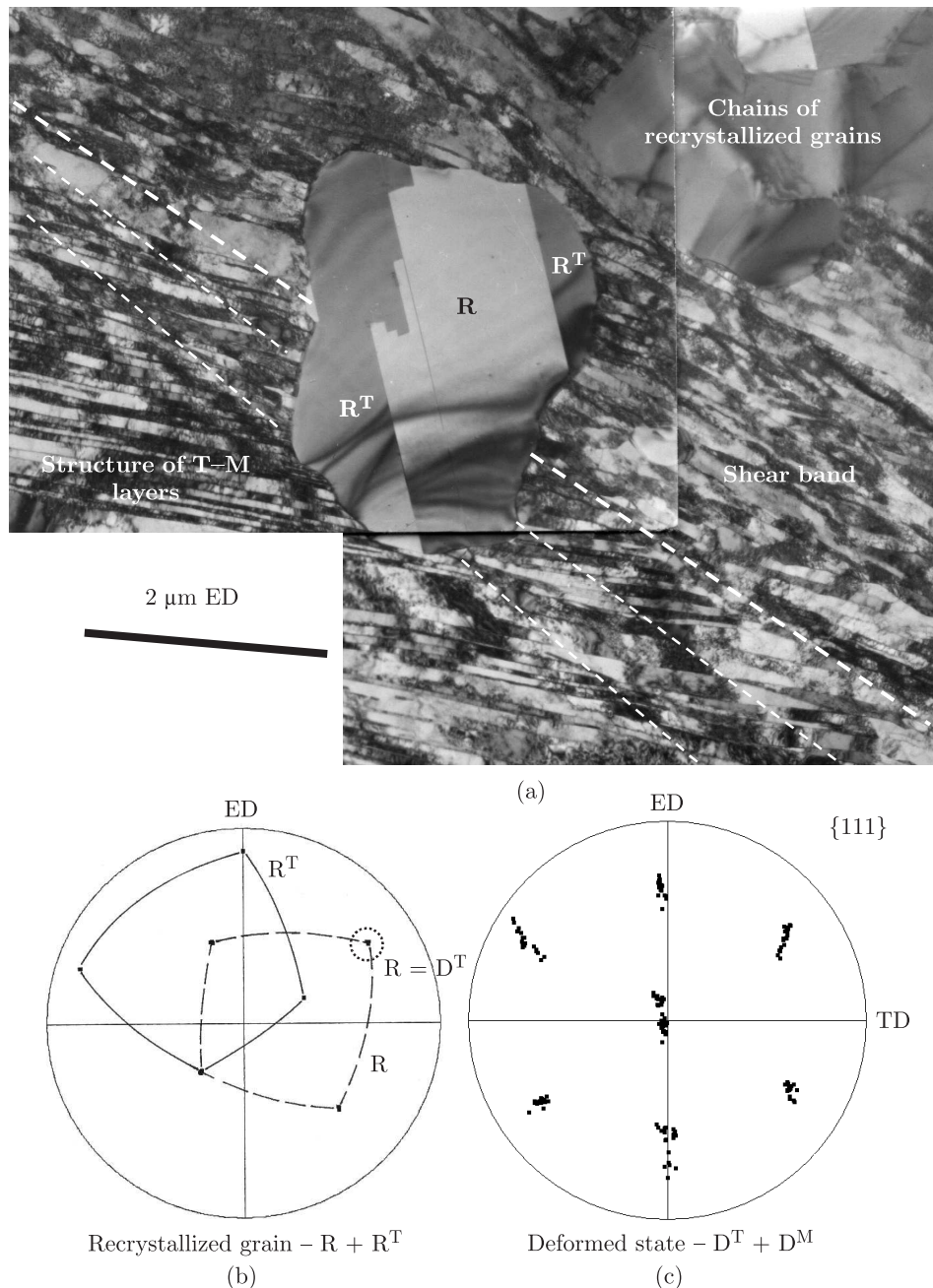


Fig. 8. Twinning of recrystallized nuclei in copper deformed 80% at 77 K and annealed 300 s at 265°C. (a) TEM microstructure, (b) and (c) $\{111\}$ pole figures showing orientations of the recrystallized grain (R), twinned (R^T) and deformed areas ($D^M + D^T$), respectively

The magnitude of the RT mechanism is confirmed by a semi-statistical analysis of the new nuclei orientations of the first recrystallized grains formed within SB microstructure. Figure 9a shows the recrystallization process within a SB microstructure. The $\{111\}$ pole figure (Fig. 9b), made up from many hundred measurements of the local orientations by the TEM, contains only the orientations of the new grain nuclei appearing inside the MSB areas. The main components of this microtexture are identified as predominantly twin related grains, but also show clearly two major components from the surroundings, i.e. $G\{110\}\langle 001\rangle$ and $\{114\}\langle 221\rangle$. These components obviously come from the internal microtexture of SBs in the deformed

state. Additionally, some near-S $\{421\}\langle 112\rangle$ oriented grains are frequently observed. The appearance of different variants of S components may be correlated with the occurrence of the rotational mechanism at the very early stages of the recrystallization process. This result again clearly indicates the importance of the $\sim 30^\circ\langle 111\rangle$ relation, as suggested in recent publications [7,8,19]. The $\sim 30^\circ\langle 111\rangle$ orientation relation should also be taken into consideration when interpreting the relatively high densities of $\Sigma 3(60^\circ\langle 111\rangle)$ grain boundaries, observed between recrystallized grains. This is often taken as proof of recrystallization twinning at the growth stages, but could well be a consequence of the fact that opposite rotations

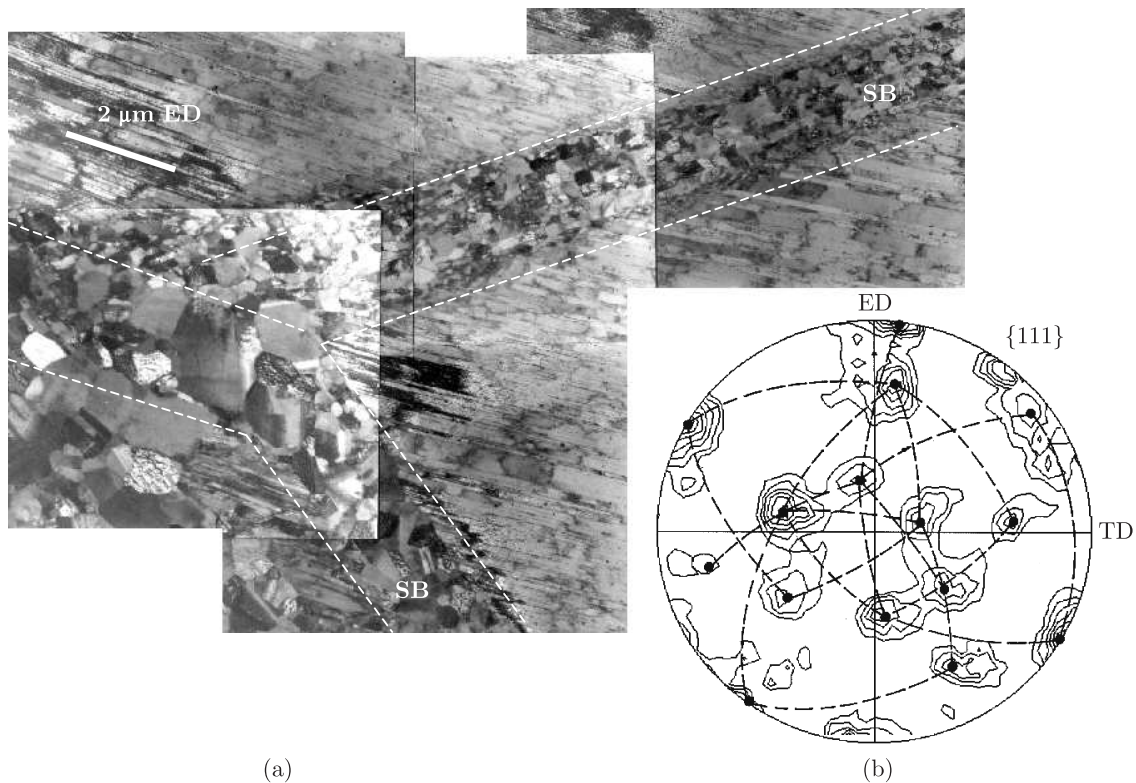


Fig. 9. (a) TEM microstructure showing spontaneous recrystallization within SB at room temperature, (b) continuous form of $\{111\}$ pole figure from TEM local orientation measurements only within nuclei of recrystallized grains. Room temperature aged

of two as-deformed regions by 30° about the same $\langle 111 \rangle$ axis also result in the occurrence of a twin relation between the recrystallized areas. It turns out that it is difficult to separate RT and $30^\circ \langle 111 \rangle$ mechanisms from chains of nuclei orientations or from measurements of the global texture. It is suggested that previous statistical analyses cannot give a definitive explanation of the crystallographic mechanism responsible for the early stages of recrystallization texture formation.

4. Discussion

All observed cases of recrystallization begin in the zones with the highest stored energy (the MSB areas) and the first-formed nuclei possess orientations strictly connected with orientations identified inside the MSB. As recrystallization proceeds, the successful new grains have well defined crystallographic relations with the surrounding twinned matrix, in which growth occurs [7,8,19]. In all observed cases, areas of single, isolated nuclei (without recrystallization twins) possess a near $25\text{--}40^\circ \langle 111 \rangle \text{--} \langle 112 \rangle$ orientation relationship with the as-deformed neighbourhood in the direction of highest growth rate. In this respect our results are qualitatively different from those obtained by other authors, in particular on non-twinning systems e.g. [9–16], which show a predominance of near $40^\circ \langle 111 \rangle$ grain boundaries between deformed and recrystallized states.

4.1. Interpretation of the grain re-orientations during recrystallization. The particular role of the orientations identi-

fied within the as-deformed regions by 30° about the same $\langle 111 \rangle$ axis also result in the occurrence of a twin relation between the recrystallized areas. It turns out that it is difficult to separate RT and $30^\circ \langle 111 \rangle$ mechanisms from chains of nuclei orientations or from measurements of the global texture. It is suggested that previous statistical analyses cannot give a definitive explanation of the crystallographic mechanism responsible for the early stages of recrystallization texture formation.

fied within the as-deformed SB has been analysed in a more quantitative manner by examining the orientation distribution of the grains using SEM/EBSD measurements [7]. A quantitative analysis of the orientations of the first formed, recrystallized grains clearly shows that the presence of the SB microtexture components within the primary recrystallized grain microtextures is a direct result of an increase of the intensities of particular poles as rotation axes. This behaviour is also clearly observed in the present work (see Figs. 5d and 5f) and indicates the particular role, during recrystallization, of certain orientations situated at the limit of the range of the deformation microtexture. In the as-deformed state these SB orientations are only weakly visible on the 'global' deformation texture and are located at the limit of their spread (Fig. 10). In the early stages of primary recrystallization, these $\langle 111 \rangle$ poles gradually become sharper. As recrystallization proceeds and $25\text{--}40^\circ \langle 111 \rangle$ or $\langle 112 \rangle$ rotations are developed in some areas of the bands, the intensity of the $\langle 111 \rangle$ pole of the most active $\{111\}$ planes during deformation systematically increases. In this way for Goss-oriented areas, the most observed position of twins within the deformed state, the intensities of all four $\langle 111 \rangle$ poles of the dominant, as-deformed orientations increase at a new position, characterised by an additional (+)TD rotation (i.e. the position of the main SB microtexture components). These observations, sometimes taken as confirmation of the ON model, are in fact due to the retention of particular $\langle 111 \rangle$ poles of the deformed state in new positions, only slightly deviated from the previous maxima by $\alpha \langle 111 \rangle$ or $\langle 112 \rangle$ rotations, and which correspond to the re-

crystallized grains. In the case of the Goss orientation, which occurs frequently in the deformed state, slip can occur on all $\{111\}$ planes and it is therefore possible to observe all four $\langle 111 \rangle$ poles corresponding to the Goss position within the recrystallized microtexture, but as rotation axes. In the near $\{111\}\langle 112 \rangle$ oriented areas, usually observed in the 'old shear bands', the $\langle 111 \rangle$ pole parallel to ND completely disappears, whereas the other three poles of the active slip systems during deformation, are relatively strongly represented within the recrystallization texture. These local orientation observations again underline the existence of a specific orientation relationship of $30^\circ \langle 111 \rangle$ type and also illustrate the difficulty of interpreting recrystallization textures from global X-ray measurements.

Generally this idea is in agreement with an old suggestion, the so-called micro-growth selection initially proposed by Ibe

and Lücke [5], where the formation of nuclei of the right orientation for growth was the result of growth selection between a variety of nuclei formed close to each other. Duggan *et al.* [12] adopted this combined ON/OG model for the particular case of the cube texture formation in high purity copper.

The $40^\circ \langle 111 \rangle$ -type orientation relationship (OR), most often discussed in literature, introduces small complications into this interpretation. Namely, this kind of OR with respect to one as-deformed component implies the occurrence of another OR type with respect to the second one, and the conditions for 'consumption' of the T-M layers are significantly different. Privileged growth into both the twin and matrix layers requires a misorientation axis parallel to the twinning plane normal and a misorientation angle of 30° , as often observed in this study and in previous work by some of the present authors, e.g. [7,8,19].

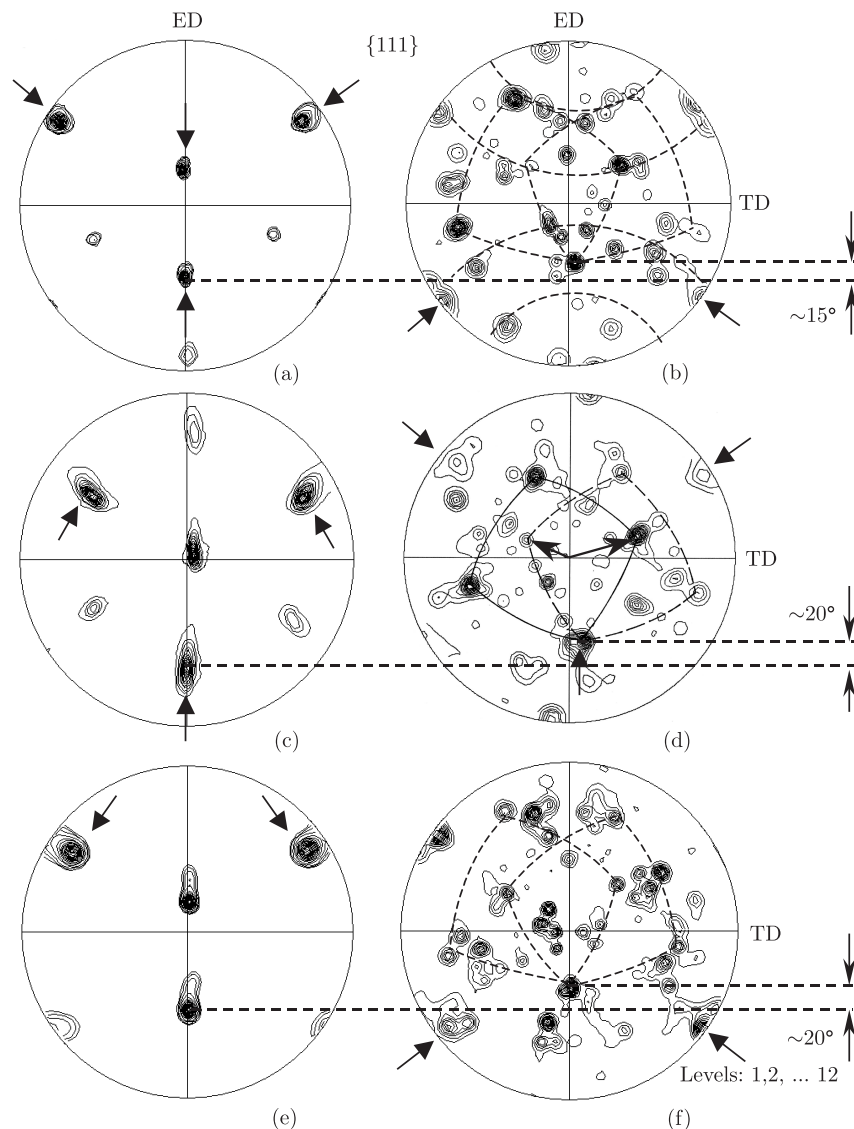


Fig. 10. Continuous $\{111\}$ pole figures re-calculated from SEM/EBSD orientation measurements showing the orientation relations between deformed, twinned matrix and new grains. (a), (c) and (e) only deformed state orientations and (b), (d) and (f) only recrystallized grains orientations. Ag samples deformed 32% at room temperature (a) and annealed 30 s at 300°C (b), Ag deformed 67% at room temperature (c) and annealed 30 s at 265°C (d) and Cu-2%Al alloy deformed at 77 K (e) and annealed 60 s at 460°C (f)

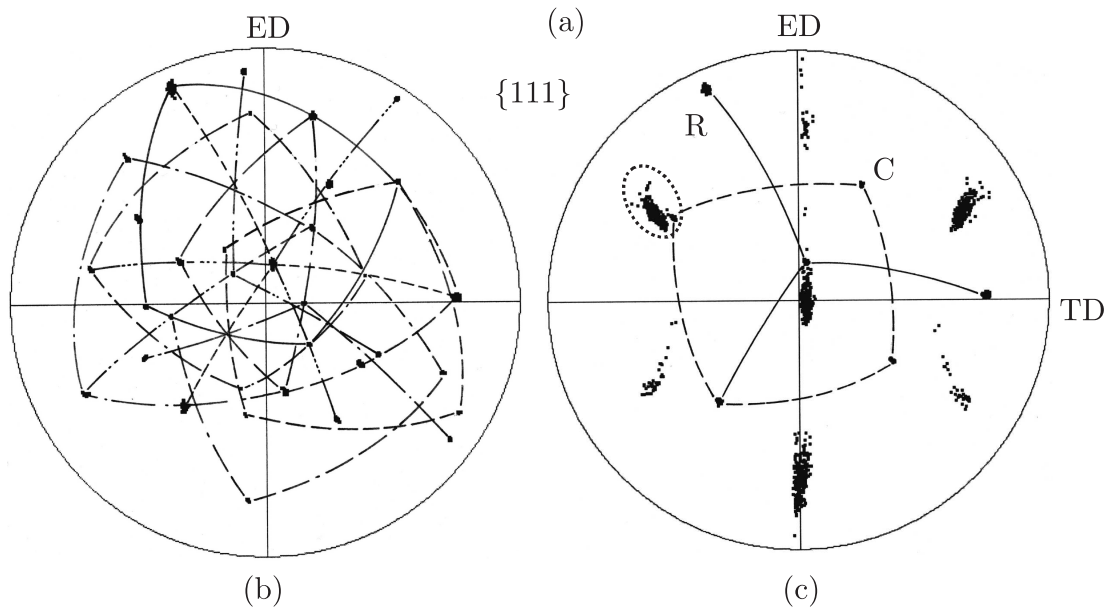
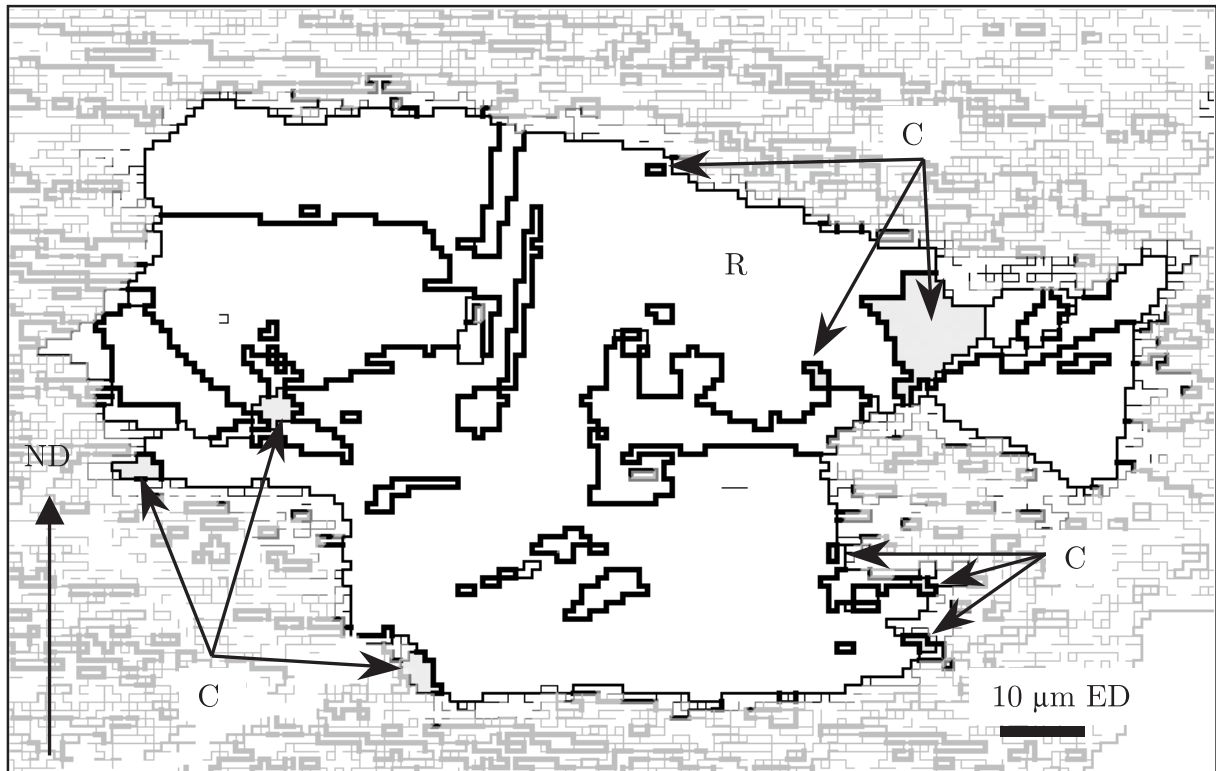


Fig. 11. Typical example of near cube grain formation as a result of recrystallization twinning, (a) part of the orientation map and (b) $\{111\}$ pole figure showing only the recrystallized orientations, (c) the orientations of the cube-oriented and R (twin to the cube) areas against a background of the deformed state orientations. Open circles on (b) and (c) show the position of the twin plane normals in the recrystallized state. SEM/EBSD measurements

The dislocation mechanism responsible for the recrystallization process remains still unresolved. From the mechanical point of view, the observed rotation of the crystallographic lattice about the $\langle 111 \rangle$ pole (inside the recrystallizing area) can be accomplished by slip on $\{112\}\langle 110 \rangle$ type slip systems, but this is not expected to occur in fcc metals deformed at room temperature since it would involve very large energy barriers.

Another, more plausible way to account for the observed rotation is based on the mechanisms of twist boundary formation. In this process the rotation vector is perpendicular to the boundary plane [20]. To form such a boundary, a thermally activated dislocation motion via screw components is necessary. In particular, the movement of two, orthogonal sets of pure screw dislocations on the same slip plane leads to the forma-

tion of a twist boundary. The result is that the crystal above the slip plane rotates with respect to the part lying below. In the general case, when this type of boundary is formed by the motion of dislocations in non-orthogonal directions, the dislocations would not be ideal screw dislocations [7].

The occurrence of $\langle 112 \rangle$ directions as rotation axes in the process of primary nuclei formation obviously again suggests a link with the deformation process (see Fig. 6a) and in particular with strong activity on a single $\{111\}\langle 011 \rangle$ system. In particular, this is clearly visible within the SBs where the nucleation occurs preferentially. Once formed the new grains exhibit a strong tendency to grow by forming new grain boundaries through recrystallization twinning and hence change their orientation. Presented in Fig. 6d, a schematic pole figure for a transition from the as-deformed orientations to the nucleus orientation by rotation $\sim 30\text{--}35^\circ \langle 112 \rangle$ is in quite good agreement with the observations, i.e. experimentally obtained new grain orientation.

As recrystallization proceeds, the importance of twinning radically increases and this is the next step in the recrystallized phase growth. This mechanism very quickly disturbs the primary orientation relationship between new grains and the as-deformed areas. However, no more than third order twins (with respect to the primary nuclei) were observed. This is enough for the almost random texture formation. In some particular cases, this multiple twinning can lead the grains orientation into positions which are twin related with respect to the as-deformed state components. Finally, this mechanism explains the possibility of the occurrence within the chains of the growing grains of the areas nearly twin related to the deformed state. However, the twin relation between the deformed areas and the single, isolated grains of uniform orientation has never been observed in this work. Also the grains which retain the orientation from the deformed state were not observed.

4.2. The occurrence of the cube-oriented grains. Cube-oriented grains, i.e. within 15° of $\{100\}\langle 001 \rangle$, occur only occasionally in the present study. This process appears to be exclusively related to recrystallization twinning. Small cube-oriented areas are twin-related to the large ones which have a primary orientation relationship of $\alpha(\langle 111 \rangle$ or $\langle 112 \rangle$)-type, with respect to one of the two groups of components describing the deformed state. It is possible to show that from areas with the primary relation between deformation substructure and recrystallized grains, an RT mechanism leads to other orientations including near-cube positions.

Thus it is clearly shown in Fig. 11a, that the cube-oriented areas are twin-related to a large part of the grain, described as R which possesses a primary orientation relationship (OR) [near $25\text{--}40^\circ(\langle 111 \rangle\text{--}\langle 112 \rangle)$] with respect to the group of components described by the D^T of the deformed microstructure. However, a detailed analysis of the orientations of particular recrystallized areas clearly shows (Figs. 11b and 11c) that it is possible to classify the R-oriented areas as primary nuclei. The other orientations are only twin related. For simplicity Fig. 11c shows only two twin related orientations R and cube, against the background of the as-deformed orientations.

5. Conclusions

The influence of the twinned microstructure of shear bands formed in copper, silver and copper base alloys crystals on the recrystallization behaviour has been studied in detail by means of TEM and SEM local orientation measurements. The microstructure and microtexture changes accompanying the early stages of recrystallization of the C-oriented crystals could be explained in terms of nucleation from specific microtexture components of the shear bands and the slip system activity during deformation. This indicates the validity of the micro-growth selection mechanism. With regard to nucleation and grain growth within twinned structures of the present metals the following conclusions can be drawn.

- For all cases of recrystallization nucleation, the critical role of dislocation slip on the most active slip systems of the microtexture components of the shear bands has been demonstrated.
- The starting points for nucleation of new grain orientations are the components of the as-deformed state. As recovery proceeds and dislocations are removed from locally recovered subgrains, the orientation changes to a frequently observed, 'equilibrium' orientation relationship of near $30^\circ \langle 111 \rangle$ type, with respect to the adjacent deformation components. This implies the occurrence, also previously observed [7,8], of a second type of misorientation near $50^\circ \langle uvw \rangle$, in accordance with the presence of the second, as-deformed, component. The freshly formed grains show a great tendency to grow by forming new grain boundaries through recrystallization twinning and hence change their orientation. The occurrence of several generations of recrystallization twins severely perturbs the primary orientation relationship.
- A quantitative analysis of the orientations of the first formed, recrystallized grains clearly shows that it is impossible to retain, within the recrystallized state, the components of the deformed state. On the one hand, this results from the clearly observed formation of the primary type of misorientation ($30^\circ \langle 111 \rangle$), between recrystallized grain of uniform orientation and the neighbouring deformed areas. On the other hand, it is shown that the presence of shear band microtexture components within the primary recrystallized grains, directly results from an increase of the intensities of the particular poles as rotation axes.

REFERENCES

- [1] R.D. Doherty, D.A. Hughes, F.J. Humphreys, J.J. Jonas, D. Juul Jensen, M.E. Kassner, W.E. King, T.R. McNelly, H.J. McQueen, and A.D. Rollet, "Current issues in recrystallization: a review", *Mat. Sci. Engn. A* 238, 219–274 (1997).
- [2] W.G. Burgers and P.C. Louwerse, "Über den Zusammenhang zwischen Deformationsvorgang und Rekrystallisationstextur bei Aluminium. (Rekrystallisation von Aluminiumeinkristallen III)", *Z. Physik* 67, 605–678 (1931).
- [3] B. Liebman, K. Lücke, and G. Masing, "Untersuchungen über die Orientierungsabhängigkeit der Wachstumsgeschwin-

- digkeit bei der primären Rekristallisation von Aluminium-Einkristallen”, *Z. Metallk.* 47, 57–63 (1956).
- [4] D.A. Molodov, U. Czubayko, G. Gottstein, and L.S. Shvindlerman, “Mobility of $\langle 111 \rangle$ tilt grain boundaries in the vicinity of the special misorientation Sigma 7 in bicrystals of pure aluminium”, *Scripta Metall. Mater.* 32, 529–534 (1995).
- [5] G. Ibe and K. Lücke, *Recrystallization, Grain Growth and Textures*, ed. by H. Margolin, Am. Soc. Metals, Metals Park, Ohio, 434 (1966).
- [6] C. Donadille, R. Valle, P. Dervin, and R. Penelle, “Development of texture and microstructure during cold-rolling and annealing of F.C.C. alloys: Example of an austenitic stainless steel”, *Acta Metall.* 37, 1547–1571 (1989).
- [7] H. Paul, J.H. Driver, and Z. Jasiński, “Shear banding and recrystallization nucleation in a Cu-2%Al alloy single crystal”, *Acta Mater.* 52, 815–830 (2002).
- [8] H. Paul, J.H. Driver, C. Maurice, and Z. Jasiński, “Crystallographic aspects of the early stages of recrystallisation in brass-type shear bands”, *Acta Mater.* 52, 4339–4355 (2002).
- [9] J. Hjelen, R. Orsund, and E. Nes, “On the origin of recrystallization textures in aluminium”, *Acta Metall. Mater.* 39, 1377–1404 (1991).
- [10] A. Berger, P.J. Wilbrandt, F. Ernst, U. Klement, and P. Haasen, “On the generation of new orientations during recrystallization: recent results on the recrystallization of tensile-deformed fcc single crystals”, *Progress in Mater. Sci.* 32, 1–95 (1988).
- [11] A.A. Ridha and W.B. Hutchinson, “Recrystallization mechanisms and the origin of cube texture in copper”, *Acta Metall.* 30, 1929–1939 (1982).
- [12] B.J. Duggan, M. Sindel, G.D. Köhlhoff, and K. Lücke, “Oriented nucleation, oriented growth and twinning in cube texture formation”, *Acta Metall. Mater.* 38, 103–111 (1990).
- [13] D. Juul Jensen, “Effects of orientation on growth during recrystallization”, in: *Microstructural and Crystallographic Aspects of Recrystallization*, ed. N. Hansen et al., Roskilde, Proceedings of 16th RISØ Int. Sym. on Mat. Sci., Denmark, 119–137 (1995).
- [14] O. Engler, “Recrystallisation textures in copper-manganese alloys”, *Acta Metall. Mater.* 49, 1237–1247 (2001).
- [15] S. Zaefferer, T. Baudin, and R. Penelle, “A study on the formation mechanisms of the cube recrystallization texture in cold rolled Fe-36%Ni alloys”, *Acta Mater.* 49, 1105–1122 (2001).
- [16] J.H. Driver, M.C. Theyssier, and C. Maurice, “Electron backscattered diffraction microtexture studies on hot deformed aluminum crystals”, *Mat. Sci. Techn.* 12, 851–858 (1996).
- [17] H. Paul, J. H. Driver, C. Maurice, and Z. Jasiński, “Shear band microtexture formation in twinned face centred cubic single crystals”, *Mat. Sci. Engn.* A359, 178–191 (2003).
- [18] H. Paul, A. Morawiec, E. Bouzy, J.J. Fundenberger, and A. Piątkowski, “Brass type shear bands and their influence on texture formation”, *Metall. Mater. Trans.* 35A, 3775–3786 (2004).
- [19] H. Paul, J.H. Driver, C. Maurice, and A. Piątkowski, “The formation of new orientations during recrystallization of silver single crystals with $\{112\}\langle 111 \rangle$ initial orientation”, *Mat. Sci. Forum* 467–470, 177–182 (2004).
- [20] F. J. Humphreys and M. Hatherly, *Recrystallization and Related Annealing Phenomena*, Pergamon Press, Oxford, 1995.